Wideband Optical Parametric Amplification of 8.375-THz WDM Signal Using Cascaded PPLN Waveguides With Reused Pump Light

Shimpei Shimizu, *Member, IEEE*, Takayuki Kobayashi, *Member, IEEE*, Takushi Kazama, Takeshi Umeki, *Member, IEEE*, Masanori Nakamura, *Member, IEEE*, Koji Enbutsu, Takahiro Kashiwazaki, Fukutaro Hamaoka, *Member, IEEE*, Munehiko Nagatani, *Member, IEEE*, Hiroshi Yamazaki, *Member, IEEE*, Kei Watanabe, and Yutaka Miyamoto, *Member, IEEE*

***Abstract*—We propose a configuration for a wideband optical parametric amplifier (OPA) using cascaded periodically poled $LiNbO_3$ (PPLN) waveguides. These PPLN waveguides have different phase-matching characteristics by controlling the temperature of each waveguide, and thus, the input wideband signal is amplified complementarily. Pump light is shared across the PPLN waveguides. As a result, pump-power-efficient gain bandwidth extension can be achieved. We numerically calculate the gain spectrum of the proposed configuration and show that the optimization of the temperature state of the 2nd PPLN modules can suppress the generation of excessive gain, resulting in a flat gain spectrum. We experimentally demonstrate an 8.7-THz amplification bandwidth (1545.32–1618.86 nm) with a >15-dB gain in the lower frequency band of the proposed OPA. We also conduct simultaneous amplification experiments with a 67-channel 125-GHz-spaced 120-Gbaud WDM signal over 8.375 THz using the proposed configuration.**

***Index Terms*—Optical fiber communication, optical parametric amplification, wavelength division multiplexing.**

I. Introduction

WIDEBAND wavelength-division multiplexing (WDM) transmission is a key technology for improving optical fiber throughput [1], [2], [3]. Expanding the amplification bandwidth of optical amplifiers is one of the major challenges to increase the transmission bandwidth. Erbium-doped fiber amplifiers (EDFAs) have been widely used in deployed WDM networks and have a ∼4.5-THz amplification bandwidth in the C- or L-bands. Broadening EDFAs to extend the conventional bands has been studied [4]. Furthermore, various wideband amplification techniques, for example, using a semiconductor amplifier [5], hybrid configuration of Raman amplification and an EDFA [6], [7], or a combination of different rare-earth-doped fiber amplifiers [8], have been studied. Multiband transmission with the S-, C-, and L-bands utilizing such wideband amplification technologies has been a recent research trend for high-capacity optical networks.

An optical parametric amplifier (OPA) utilizing nonlinear optical effects has attracted research attention because of its wide amplification bandwidth [9], [10], [11], [12], [13], [14], [15], [16]. OPAs can be used for various telecommunication bands by modifying the phase-matching characteristics of the medium and the allocation of the pump light [10], [11], [12], [13]. One additional feature of OPAs is the generation of idler light while input signal light is amplified. By using this idler light, wavelength conversion can be performed, and its application to multiband networks is being considered [11], [12]. OPAs are classified into those based on $\chi^{(3)}$-nonlinearity (e.g., fiber-based OPA) and those based on $\chi^{(2)}$-nonlinearity. Using a fiber-based OPA, a 170-nm amplification bandwidth (>20 THz) with a >10-dB phase-sensitive amplification gain was reported [9]. In an OPA using a periodically poled $LiNbO_3$ (PPLN) waveguide as a $\chi^{(2)}$-nonlinear medium, the efficiency of the unwanted nonlinear optical effects among WDM channels, which causes excessive signal degradation, is small. Therefore, the PPLN-based OPA can simultaneously amplify a WDM signal with high gain and output power. With the PPLN-based OPA, a >10-THz gain bandwidth and the potential of wideband inline WDM amplification were reported [14], [15]. Recently, over-14-THz lumped signal amplification and inline-amplified WDM transmission with an 80-km fiber span using PPLN-based OPAs were demonstrated [16]. An OPA requires a reserve band for idler light generated with signal amplification. Therefore, a single medium can amplify a half band of the gain bandwidth. In the above demonstration of 14-THz simultaneous signal

Manuscript received 2 June 2023; revised 19 July 2023; accepted 22 July 2023. Date of publication 26 July 2023; date of current version 16 December 2023. *(Corresponding author: Shimpei Shimizu.)*

Shimpei Shimizu, Takayuki Kobayashi, Masanori Nakamura, Fukutaro Hamaoka, and Yutaka Miyamoto are with the NTT Network Innovation Laboratories, NTT Corporation, Yokosuka 239-0847, Japan (e-mail: shimpei.shimizu@ntt.com; tkyk.kobayashi@ntt.com; msnr.nakamura@ntt.com; fukutaro.hamaoka@ntt.com; yutaka.miyamoto@ntt.com).

Takushi Kazama, Takeshi Umeki, Munehiko Nagatani, Hiroshi Yamazaki, and Kei Watanabe are with the NTT Device Technology Laboratories, NTT Corporation, Atsugi 243-0198, Japan, and also with the NTT Network Innovation Laboratories, NTT Corporation, Yokosuka 239-0847, Japan (e-mail: takushi.kazama@ntt.com; takeshi.umeki@ntt.com; munehiko.nagatani@ntt.com; hrsh.yamazaki@ntt.com; kei.watanabe@ntt.com).

Koji Enbutsu and Takahiro Kashiwazaki are with the NTT Device Technology Laboratories, NTT Corporation, Atsugi 243-0198, Japan (e-mail: koji.enbutsu@ntt.com; takahiro.kashiwazaki@ntt.com).

Color versions of one or more figures in this article are available at https://doi.org/10.1109/JLT.2023.3299017.

Digital Object Identifier 10.1109/JLT.2023.3299017

amplification [16], two OPAs were implemented in parallel to fully utilize the gain bandwidth of PPLNs and complementarily amplified the WDM signal; one of the OPAs amplified the signal over up to ∼7.5 THz.

In demonstrations of wideband inline amplification using a PPLN-based OPA, the effective gain bandwidth was extended by varying the quasi-phase-matching (QPM) bandwidth by controlling the temperature of the PPLN waveguide [13]. By increasing the waveguide temperature, the outside gain becomes large, but the gain near the degenerate frequency (the center of the gain band) becomes small. Therefore, bandwidth extension by controlling the waveguide temperature is maximum when the gain of channels allocated nearest the degenerate frequency is equal to the gain required to compensate for transmission loss. For further extension, an increase in the pump power is required in the conventional OPA. In addition, the gain gradient that occurs with temperature detuning results in excessive gain around the frequency with maximum gain. Unwanted output power due to such excess gain requires gain equalization with large attenuation and limits the output power performance.

This article describes our proposed configuration for optical parametric amplification using cascaded PPLN waveguides to extend the gain bandwidth without an increase in pump power [17]. Each PPLN module has different QPM characteristics due to waveguide temperature control and amplifies a wideband WDM signal complementarily. The pump light is shared across the cascaded PPLN waveguides, and thus, power-efficient bandwidth extension can be achieved. The effect of waveguide temperature on the gain spectrum is evaluated in numerical simulations with the coupled wave equation (CWE), and the optimal temperature condition for obtaining a flat gain spectrum is clarified. In addition, we experimentally measure the gain spectrum and compare that with simulation results. We also describe a demonstration involving the wideband inline amplification of a 125-GHz-spaced 67-channel 800-Gbps/λ WDM signal over 8.375 THz under a 2 × 30-km transmission condition as an application of the proposed OPA to optical networks.

II. Proposed Configuration

Fig. 1 shows the conventional and proposed configurations of the OPA using 4-port PPLN modules. The 4-port module has low-loss integrated pump (de-)combiners using dichroic filters (DFs), and its I/O interfaces are four polarization-maintaining fiber pigtails [18]. The PPLN waveguide is mounted on a copper plate. To maintain the phase-matching conditions, a Peltier device is placed under the plate to actively control and maintain the temperature of the overall waveguide [19]. Because the optical parametric amplification process is polarization sensitive, a polarization-diverse configuration is used that separately amplifies the orthogonal polarization components of the input signal [13]. We used a parallel-type configuration, which features two waveguides sandwiched by a polarization-beam splitter and combiner (PBS/PBC) [14]. In the conventional configuration shown in Fig. 1(a), one PPLN module is used per polarization-diverse arm. The optical parametric amplification process based on $\chi^{(2)}$-nonlinearity requires a second harmonic (SH) pump at

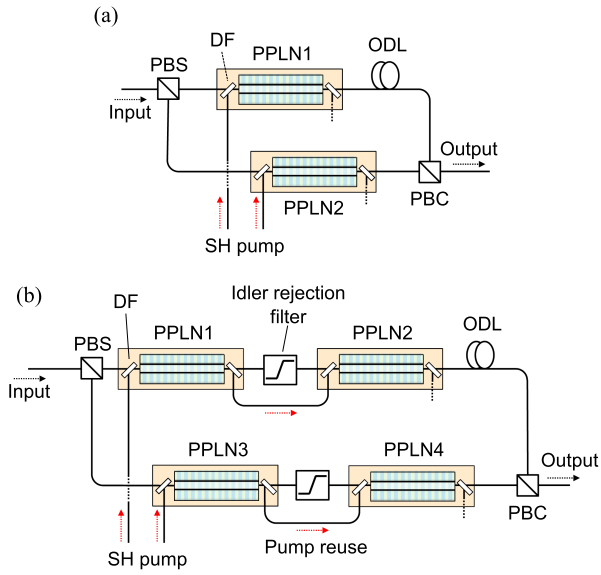

Fig. 1. (a) Conventional and (b) proposed configurations of parallel-type polarization-diverse PPLN-based OPA. PBS: Polarization-beam splitter, PBC: Polarization-beam combiner, DF: Dichroic filter, and ODL: Optical delay line.

double the frequency of the degenerate frequency (the center frequency of the QPM band). To obtain a high-power pump, continuous wave (CW) light at the degenerate frequency, f_0, and an EDFA are used. The CW light at f_0 is amplified by a high-power EDFA and is then converted to SH light at $2f_0$ by using a second-harmonic generation (SHG) process with another PPLN waveguide [20]. By using different media for SHG and optical parametric amplification, unwanted nonlinear effects that cause inter-channel crosstalk can be effectively suppressed. The SH pump is combined with signal light and then de-combined after amplification using DFs in the 4-port PPLN module. In the parallel-type polarization-diverse configuration, an optical delay line (ODL) is used to compensate for the difference in the optical path length between two polarization-diverse arms. In the conventional configuration, the gain characteristics are restricted by the performance of a single medium.

Fig. 1(b) shows our proposed configuration for further wideband amplification. Two 4-port PPLN modules are cascaded in one polarization-diverse arm. An optical filter is placed between the two cascaded modules to eliminate the idler light generated in the 1st PPLN modules (PPLN1&3). This is to avoid interference between signals and idlers in the 2nd modules (PPLN2&4). When the proposed configuration is used as a wavelength converter or an optical phase conjugator, the original signal light is eliminated instead of the idler light. The SH pump is reused by connecting the pump-output port of the 1st modules to the pump-input port of the 2nd modules.

To describe the operational details of the proposed configuration, we first discuss the gain bandwidth of the PPLN waveguide. The gain of optical parametric amplification in the PPLN waveguide without pump depletion and absorption in the waveguide is given as

$$G = \cosh^2(gL) + \left(\frac{\Delta\beta}{2g}\right)^2 \sinh^2(gL), \tag{1}$$

where g is the gain factor, $\Delta\beta$ is the amount of phase mismatch, and L is the length of the waveguide [21]. The g is expressed as

$$g \equiv \sqrt{\kappa_{\rm s}\kappa_{\rm i}P_{\rm p} - \left(\frac{\Delta\beta}{2}\right)^2}, \tag{2}$$

where $P_{\rm p}$ is the power of the SH pump. The suffixes of s, i, and p indicate signal, idler, and SH pump components, respectively. κ is a coefficient representing the efficiency of the $\chi^{(2)}$-nonlinear optical process, and $(\kappa_0 L)^2$ represents the SHG efficiency of the waveguide. $\kappa_{\rm s}$ which is κ at the signal frequency is expressed as $(\omega_{\rm s}/\omega_0)\kappa_0$. The relation of the angular frequencies is $\omega_{\rm p} = 2\omega_0 = \omega_{\rm s} + \omega_{\rm i}$. The effective $\Delta\beta$, which includes the effect of periodic poling, is expressed as

$$\Delta\beta = \frac{1}{c}\left[n\left(\omega_{\rm p}\right)\omega_{\rm p} - n\left(\omega_{\rm s}\right)\omega_{\rm s} - n\left(\omega_{\rm i}\right)\omega_{\rm i}\right] - \frac{2\pi}{\Lambda}, \tag{3}$$

where n is the effective refractive index of a fundamental mode in the PPLN waveguide, c is the speed of light, and Λ is the poling period of the PPLN waveguide [22]. In the case that the phase-mismatch is large, that is, $\{\kappa_s\kappa_i P_p - (\Delta\beta/2)^2\} < 0$, g is replaced with

$$jg' \equiv j\sqrt{\left(\frac{\Delta\beta}{2}\right)^2 - \kappa_{\rm s}\kappa_{\rm i}P_{\rm p}}, \tag{4}$$

and the analytical solution for the amplification gain is then given as:

$$G = 1 + \frac{\kappa_{\rm s}\kappa_{\rm i}P_{\rm p}}{g'^2}\sin^2\left(g'L\right). \tag{5}$$

These equations indicate that the gain depends on the refractive index spectrum of the waveguide. The refractive index spectrum of $LiNbO_3$ is expressed by the Sellmeier equation and is temperature dependent [23]. That is, the $\Delta\beta$ is expressed as a function of the waveguide temperature, T,

$$\Delta\beta = \frac{1}{c}\left[n\left(\omega_{\rm p}, T\right)\omega_{\rm p} - n\left(\omega_{\rm s}, T\right)\omega_{\rm s} - n\left(\omega_{\rm i}, T\right)\omega_{\rm i}\right] - \frac{2\pi}{\Lambda}. \tag{6}$$

Thus, the gain spectrum can be varied by controlling the waveguide temperature. Fig. 2 shows an example of calculating the dependences of $\Delta\beta$ and the gain spectrum on the waveguide temperature using the above equations. The calculation parameters were as follows: $f_0 = 194.0$ THz, $L = 45$ mm [19], $P_{\rm p} = 1.7$ W, the optimal temperature for f_0 was 50 °C, and the SHG efficiency was 820%/W [19]. Λ was optimized for f_0 at 50 °C (∼18.6 μm), i.e., $\Delta\beta(\omega_0, 50\ ^\circ\mathrm{C}) = 0$. The refractive index spectrum of a PPLN was calculated on the basis of [23]. The effective refractive index of a fundamental mode propagating in the PPLN waveguide was assumed to be equal to the refractive index of the material. At the waveguide temperature, $T = 50$ °C, which was the optimal temperature for f_0, a flat top gain spectrum was observed around f_0. By increasing the waveguide temperature to 52 °C, the outer gain increases while the inner gain around f_0 decreases, and the effective gain bandwidth can be extended. Wideband optical parametric inline amplification was demonstrated with this temperature detuning [16]. In an application as a wideband inline amplifier for multi-span WDM transmission, the effective gain bandwidth is maximized when

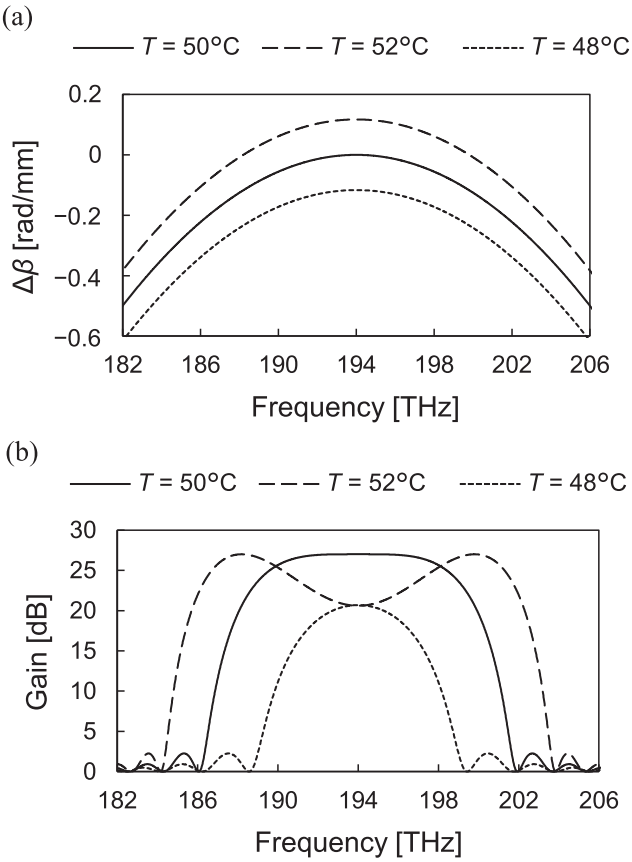

Fig. 2. Calculation results for dependence of (a) $\Delta\beta$ and (b) gain spectrum on waveguide temperature.

the gain around f_0 is the gain required to transmit the signal. As the waveguide temperature continues to increase further, the effective gain bandwidth narrows because the inner band around f_0 hollows out faster than the outer band expands. Therefore, to further extend the effective gain bandwidth, the power of the pump light must be increased. Meanwhile, at a low temperature, $T = 48$ °C, there were no frequencies at which $\Delta\beta = 0$, the overall gain was reduced, and the gain spectrum was sharpened.

In the proposed configuration, the waveguide temperature of the 1st PPLNs is controlled to extend the gain spectrum, as shown in the high temperature state in Fig. 2. The 2nd PPLNs (PPLN2&4) amplify the small gain band of the 1st PPLNs (PPLN1&3) around f_0. With this complementary amplification, further temperature detuning of the 1st PPLNs becomes possible, and extension of the effective gain bandwidth is achieved. The signal amplified by the 1st PPLN modules is passed through an optical filter to reject idler light and is then re-combined with the SH pump light in the 2nd modules. The de-combined pump light in the 1st PPLN modules is input to the 2nd PPLN modules, resulting in an extended the effective gain bandwidth without increasing power consumption. The gain spectrum of the 2nd PPLNs is set to a narrow bandwidth around f_0 by detuning the waveguide temperature opposite that of the 1st PPLNs, as shown in the low-temperature condition in Fig. 2. The narrow gain bandwidth of the 2nd PPLNs prevents unwanted excessive gain at the frequencies at which the gain spectra of the 1st PPLNs and

2nd PPLNs intersect. Therefore, the gain saturation due to pump depletion for the excessive gain (excessive output power) can be suppressed. The outer bands that are not amplified by the 2nd PPLN modules are subject to transmission loss in the 2nd PPLN modules. Therefore, the transmission loss of the 2nd PPLN modules is an important parameter for effectively extending the gain bandwidth. Recently, we developed an ultra-low-loss PPLN waveguide fabricated by a mechanical sculpturing technique, and the transmission loss of the 45-mm-long waveguide was ∼0.32 dB at 1545 nm [19]; that of our waveguide fabricated by a dry-etching technique was ∼1.00 dB [18].

When the OPA amplifies the entire band of a WDM signal with a large gain, the wavelength dependence of the noise figure (NF) is negligible [13]. However, in the proposed configuration, the frequency dependence of NF becomes apparent in the band where the gain of the 1st PPLN modules is small, due to optical losses between the 1st and 2nd PPLNs. Assuming that the NF spectrum of the conventional OPA is the reference, the NF penalty in the proposed OPA is expressed as

$$\Delta N\left(f\right) \approx 1 + \frac{1}{N_{\mathrm{ref}}\left(f\right)}\left(\frac{1}{G_{1\mathrm{st}}\left(f\right)} - \frac{1}{G_{\mathrm{ref}}\left(f\right)}\right) + \frac{N_{2\mathrm{nd}}\left(f\right)}{N_{\mathrm{ref}}\left(f\right)\cdot l_{\mathrm{filter}}\left(f\right)\cdot G_{1\mathrm{st}}\left(f\right)}, \tag{7}$$

where $l_{\mathrm{filter}}(f)$ is the loss spectrum of the idler filter, $N_{\mathrm{ref}}(f)$ is the NF with a large-gain OPA, $G_{1\mathrm{st}}(f)$ and $G_{\mathrm{ref}}(f)$ are the gain spectra of the 1st PPLN modules in the proposed OPA and conventional OPA, respectively, and $N_{2\mathrm{nd}}(f)$ is the NF of the 2nd PPLN modules in the proposed OPA.

III. Amplification Characteristics

This section describes the amplification characteristics of the proposed configuration. First, we evaluate the dependence of a gain spectrum on the waveguide temperature of the 2nd PPLNs in the proposed configuration in numerical simulations using the CWE. We clarify the temperature condition for obtaining a flat gain spectrum. Next, we experimentally measure the gain spectrum of the proposed configuration using the 4-port PPLN modules, and we also compare that with the results of numerical simulations.

A. Simulation Modes

We calculated the CWE to verify the gain spectrum of the proposed configuration. The CWE (described by one-dimensional scalar wave equations) of the $\chi^{(2)}$-based optical parametric amplification process in the PPLN waveguide is given as [21]:

$$\frac{dE_{\mathrm{s}}\left(z\right)}{dz} = -\frac{\alpha_{\mathrm{s}}}{2}E_{\mathrm{s}}\left(z\right) + j\kappa_{\mathrm{s}}E_{\mathrm{p}}\left(z\right)E_{\mathrm{i}}^{*}\left(z\right)\exp\left[j\Delta\beta z\right], \tag{8}$$

$$\frac{dE_{\mathrm{i}}\left(z\right)}{dz} = -\frac{\alpha_{\mathrm{i}}}{2}E_{\mathrm{i}}\left(z\right) + j\kappa_{\mathrm{i}}E_{\mathrm{p}}\left(z\right)E_{\mathrm{s}}^{*}\left(z\right)\exp\left[j\Delta\beta z\right], \tag{9}$$

$$\frac{dE_{\mathrm{p}}\left(z\right)}{dz} = -\frac{\alpha_{\mathrm{p}}}{2}E_{\mathrm{p}}\left(z\right) + j\kappa_{\mathrm{p}}E_{\mathrm{s}}\left(z\right)E_{\mathrm{i}}\left(z\right)\exp\left[-j\Delta\beta z\right], \tag{10}$$

where E_{s}, E_{i}, and E_{p} are complex amplitudes of signal, idler, and pump light. The CWE was deformed to equations for the real amplitude, A, of each light as:

$$\frac{dA_{\mathrm{s}}\left(z\right)}{dz} = -\frac{\alpha}{2}A_{\mathrm{s}}\left(z\right) + \kappa A_{\mathrm{p}}\left(z\right)A_{\mathrm{i}}\left(z\right)\sin\left[\theta\left(z\right)\right], \tag{11}$$

$$\frac{dA_{\mathrm{i}}\left(z\right)}{dz} = -\frac{\alpha}{2}A_{\mathrm{i}}\left(z\right) + \kappa A_{\mathrm{p}}\left(z\right)A_{\mathrm{s}}\left(z\right)\sin\left[\theta\left(z\right)\right], \tag{12}$$

$$\frac{dA_{\mathrm{p}}\left(z\right)}{dz} = -\frac{\alpha}{2}A_{\mathrm{p}}\left(z\right) - 2\kappa A_{\mathrm{s}}\left(z\right)A_{\mathrm{i}}\left(z\right)\sin\left[\theta\left(z\right)\right], \tag{13}$$

$$\frac{d\theta\left(z\right)}{dz} = \kappa\left(\frac{A_{\mathrm{p}}\left(z\right)A_{\mathrm{i}}\left(z\right)}{A_{\mathrm{s}}\left(z\right)} + \frac{A_{\mathrm{p}}\left(z\right)A_{\mathrm{s}}\left(z\right)}{A_{\mathrm{i}}\left(z\right)} - 2\frac{A_{\mathrm{s}}\left(z\right)A_{\mathrm{i}}\left(z\right)}{A_{\mathrm{p}}\left(z\right)}\right)\cos\left[\theta\left(z\right)\right] - \Delta\beta\left(z\right). \tag{14}$$

The transformation of CWE was adapted from [24], [25]. For calculating the gain characteristics in the frequency domain, (11)–(14) were simultaneously calculated with a 1-GHz resolution. The pump light was assumed to consist of the single frequency of ω_{p}. In addition, we neglected the frequency dependence of the SHG efficiency and propagation loss of the waveguide (i.e., $\kappa = \kappa_{\mathrm{s}} = \kappa_{\mathrm{i}} = \kappa_{\mathrm{p}}/2$ and $\alpha = \alpha_{\mathrm{s}} = \alpha_{\mathrm{i}} = \alpha_{\mathrm{p}}$). The simulation parameters were as follows: the step size of the propagation was 0.1 μm, the length of the waveguide was 45 mm, the insertion loss of the PBS/PBC was 1.0 dB, the coupling loss between the waveguide and fibers was 0.5 dB, and the loss of the idler rejection filter was 0.3 dB. In the previous section, Λ was optimized for f_0 (= 194.0 THz) at 50 °C. The κ and α of the waveguide in the 1st modules assumed to be fabricated with a dry etching technique were 1200%/W and 0.022 dB/mm, respectively [18]. Those of the low-loss 2nd modules assumed to be fabricated with a mechanical sculpturing technique were 820%/W, and 0.007 dB/mm, respectively [19]. Note that, the propagation of each light was calculated with nonlinear coefficients of constant sign, assuming that the phase relation between the signal, idler, and pump lights was changed with the effective $\Delta\beta$ shown in (3). In addition, we ignored a contribution of amplified quantum noise to the output power, induced by the conversion of a vacuum fluctuation at the idler frequency to the signal frequency (i.e., $A_{\mathrm{i}}^{2}(0) = 0$).

B. Gain and NF Spectra

Fig. 3 shows the dependence of the gain spectrum of the proposed OPA on the waveguide temperature calculated by the CWE. In this work, we set the required gain to 15 dB and assumed that the 15-dB-gain bandwidth is the effective gain bandwidth. The phase-matching state of the 1st PPLNs was fixed so that the gain at 185 THz was ∼15 dB. The input SH pump power to the 1st and 2nd PPLNs were ∼1.6 W and ∼0.6 W, respectively. These were the same power as in the experiments described below. We varied the waveguide temperature of the 2nd PPLN from 50.0 °C to 49.0 °C in 0.1 °C increments and plotted the gain spectra. Fig. 3(a) shows the gain spectrum of the 2nd PPLNs at each temperature. The gain of the 2nd PPLN modules was about 10 dB with the reused SH pump of 0.6 W around f_0. The lower the temperature, the more the gain decreased overall, and its spectrum sharpened. Fig. 3(b)

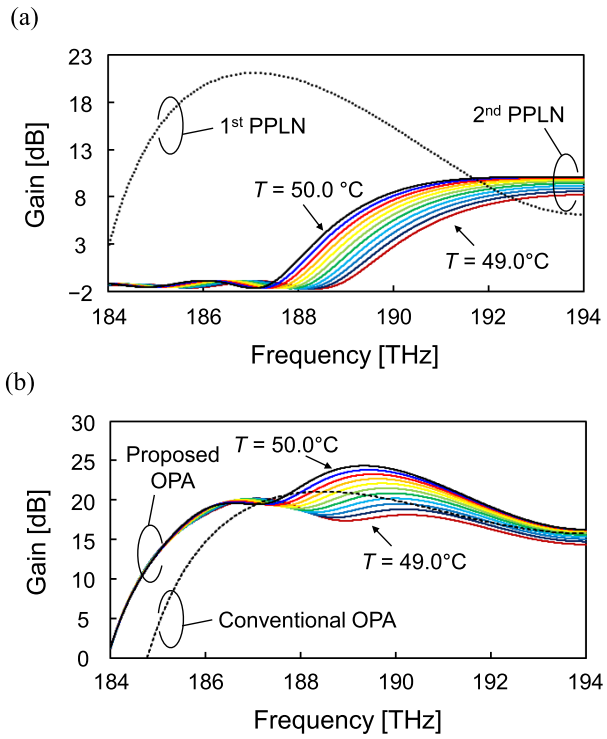

Fig. 3. Calculation results for CWE. Dependence of gain spectra of (a) 2nd PPLN module and (b) proposed OPA on waveguide temperature. Waveguide temperature was varied from 50.0 °C to 49.0 °C in 0.1 °C increments.

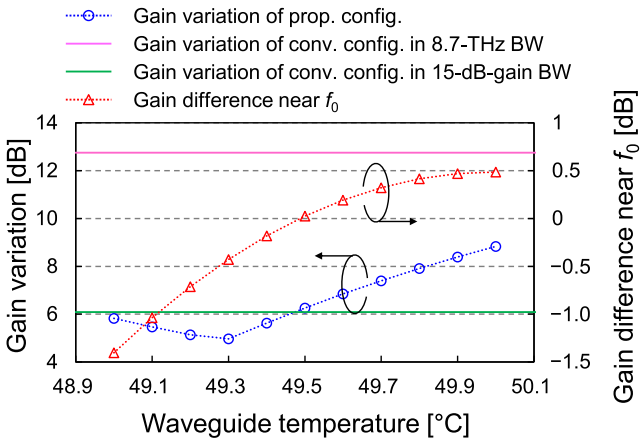

Fig. 4. Calculation results for gain variation in 8.7-THz bandwidth and gain difference between proposed and conventional configurations near f_0 as function of waveguide temperature. Solid lines indicate gain variation of conventional configuration at optimal temperature with maximized 15-dB-gain bandwidth.

shows the gain spectrum of the proposed configuration combining the 1st and 2nd PPLNs. The proposed OPA extended the 15-dB-gain bandwidth by ∼0.82 THz compared with the conventional OPA with a single PPLN module per polarization, resulting in 8.7 THz. On the other hand, as we can see, a large excess gain occurred at the intersection between the gain spectra of the 1st and 2nd PPLNs at 50.0 °C. Because such excessive gain caused the gain saturation characteristics to degrade, the gain spectra should be as flat as possible with a low waveguide temperature. Fig. 4 shows the dependence of the gain variation and gain difference between proposed and conventional configurations near f_0 on waveguide temperature. The gain variation was calculated as the difference between the maximum and minimum gains within 8.7 THz from 194 THz. For comparison, the gain variations of the conventional configuration within 8.7-THz bandwidth and 15-dB-gain bandwidth are also plotted. The gain difference is determined with the gain of the proposed configuration minus the gain of the conventional configuration near f_0 (at 193.999 THz). In the conventional configuration, the gain variation within 8.7 THz was large (12.7 dB) since the gain in the frequency band lower than 186 THz was small. Within the 15-dB-gain bandwidth, the gain variation was 6.1 dB. In the proposed configuration, the gain gradient became smaller as the temperature decreased, reaching a minimum value of 4.9 dB at 49.3 °C. At <49.2 °C, the gain gradient turned upward as the gain in the 2nd PPLN modules became too small. Meanwhile, the lower-bound temperature condition at which the gain near the degenerate frequency was comparable to that of the conventional configuration was 49.5 °C according to the gain difference plots. The gain variation of 6.2 dB at 49.5 °C was comparable to that in the 15-dB-gain bandwidth of the conventional configuration. This shows that the proposed configuration could extend the gain bandwidth without compromising the uniformity of the gain spectrum. Therefore, we attempted to control the PPLN modules in the following experiments to be close to the phase-matching state at 49.5 °C in the simulations.

We experimentally measured the gain and NF spectra for a small signal (unsaturated region) and compared them with the simulation results. Fig. 5(a) shows the measurement setup. The configuration of the conventional and proposed OPAs was polarization-diverse [14]. The spectra were measured by sweeping the wavelength of input CW light at −15 dBm with an optical spectrum analyzer (OSA). The NF was calculated by comparing the optical spectra of the CW light before and after amplification [26]. The degenerate frequency of the optical parametric amplification in the PPLN waveguides was 194.0 THz (= 1545.32 nm), the same as in the numerical simulations. The loss of the dielectric multilayer filter for idler rejection was 0.3–0.6 dB. The power of the SH pump was ∼1.6 W. As in the simulations, we defined the effective amplification bandwidth as the bandwidth at which a 15-dB gain was obtained. Fig. 5(b) and (c) show the measurement results. In the conventional OPA, the waveguide temperature was controlled so that the 15-dB gain bandwidth was the widest, and a ∼7.8-THz effective gain bandwidth from f_0 was achieved. This was in good agreement with the simulation results. In the proposed OPA, the 1st PPLNs (PPLN1&3) were detuned to increase the outside gain while the gain around f_0 was decreased by ∼10 dB. The 2nd PPLNs (PPLN2&4) consisted of low-loss PPLN waveguides fabricated with mechanical sculpturing [19] to suppress the gain reduction in the outer-band components and had a gain only in the band around f_0. The SH pump of ∼0.6 W could be input to the 2nd modules through de-combination with the signal in the 1st modules and the connection by fiber patch cords. Comparison with the simulation showed good agreement with the results at about 49.45 °C as shown by the solid line. Thus, a ∼8.7-THz effective gain bandwidth was achieved from 194.0 to 185.3 THz with a

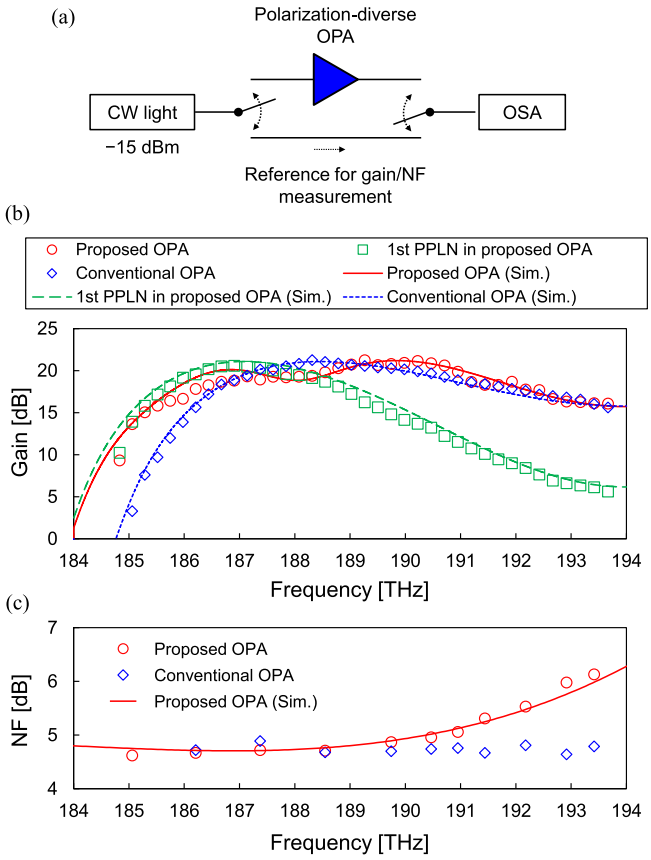

Fig. 5. Experimental measurement of gain and NF spectra. (a) Experimental setup. (b) Gain spectra. (c) NF spectra.

>15-dB gain, and the proposed OPA extended the 15-dB-gain bandwidth by ∼0.9 THz without an increase in pump power. The maximum NF penalty was 1.4 dB, and the NF spectrum was in good agreement with the theoretical value calculated with (7).

IV. 8.375-THz Simultaneous Optical Inline Amplification in 2 × 30-km WDM Transmission Condition

We performed a transmission experiment with a wideband WDM signal as an application of the proposed configuration to optical fiber networks. A 125-GHz-spaced 67-channel WDM signal over 8.375 THz from 185.187 to 193.562 THz (1548.81–1618.86 nm) was inline amplified by the proposed OPA in a 2 × 30-km transmission condition, and the modulation format was 120-Gbaud dual-polarization (DP) probabilistically shaped (PS) 36QAM, of which the net data rate was 800 Gbps. Through this experiment, we show that high-order QAM signals with a high-symbol rate can be amplified without the distortion caused by the proposed OPA in the unsaturated region.

A. Experimental Setup

Fig. 6(a) shows the experimental setup for the 2 × 30-km transmission of a 125-GHz-spaced 67-channel WDM signal using the proposed OPA. The OPA was used for an inline amplifier of the 8.375-THz WDM signal. On the transmitter side, a Nyquist-pulse-shaped 120-Gbaud PS-36QAM signal with a roll-off factor of 0.03 was generated using an I/Q modulator driven by analogue-multiplexer-based high-speed digital-to-analogue convertors (AMUX-based DACs) [27]. Then, the optical signal was polarization-multiplexed by a polarization-division multiplexing emulator (PDME). The entropy of the DP-PS-36QAM signal was 8.87 bits per 4D symbol. The interference WDM channels were emulated using amplified spontaneous emission (ASE) from C- and L-band EDFAs [28]. Fig. 6(b) shows the fiber-launched spectrum of the WDM signal. The interference WDM signal was spectrally shaped and combined with the channel under test (CUT) using a wavelength selective switch (WSS), and an 8.375-THz WDM signal was generated from 185.187 THz (1618.859 nm) to 193.562 THz (1548.815 nm). The interference WDM signal was rectangularly hollowed out around the wavelength of the CUT with a 125-GHz bandwidth in the WSS. The transmission lines were 30-km G.654.E single-mode fibers with a ∼6-dB propagation loss. The average fiber-launched optical power was −16.5 dBm/ch. (total power was 1.8 dBm), and it was limited by the output power of the ASE source for dummy WDM channels. The total input power to the proposed OPA was −5.0 dBm (−23.2 dBm/ch.), at which the gain saturation was sufficiently small. The output power from the OPA was 14.7 dBm (−3.5 dBm/ch.). In frequency bands where the extinction ratio of the idler rejection filter, that is, the power ratio between the passing signal component and the rejected idler component, is not sufficient, interference between the signal component and the wavelength-converted idler component in the 2nd PPLN may result in degradation of the signal quality. Therefore, we used a frequency band with an extinction ratio of >30 dB and cut off the frequency band with a low extinction ratio around f_0. A guard band of ∼0.3 THz from f_0 was required, which limited the bandwidth of the WDM signal to 8.375 THz, although the gain bandwidth of the proposed OPA was 8.7 THz. To suppress polarization-mode dispersion (PMD), we measured the optical path lengths of two polarization-diverse arms and adjusted the variable ODL in the OPA so that the difference between them was less than 0.1 mm, corresponding to a PMD of ∼0.5 ps. For absolutely achieving zero PMD, a configuration has been proposed in which the phase drift between two polarization-diverse arms is actively compensated for by using a piezoelectric transducer-based fiber stretcher [29]. However, even in our configuration without such active control, the PMD was low thanks to the accurate optical path length adjustment using the variable ODL, and its drift was slow compared with the symbol rate, enough to be compensated for by the receiver digital signal processing. After transmission, the CUT was pre-amplified by a C- or L-band EDFA, extracted by a band-pass filter (BPF), and received by a coherent receiver. The received CUT was digitized using a digital storage oscilloscope operating with 256 Gsample/s and was demodulated by offline digital signal processing. The digitized signal was resampled to 2 samples/symbol, and a frequency-domain fixed equalizer compensated for chromatic dispersion. Then, the symbol was demodulated with a complex 8 × 2 adaptive equalizer updated by a decision-directed and pilot-aided least-mean-square algorithm [30]. Normalized generalized mutual information (NGMI) was

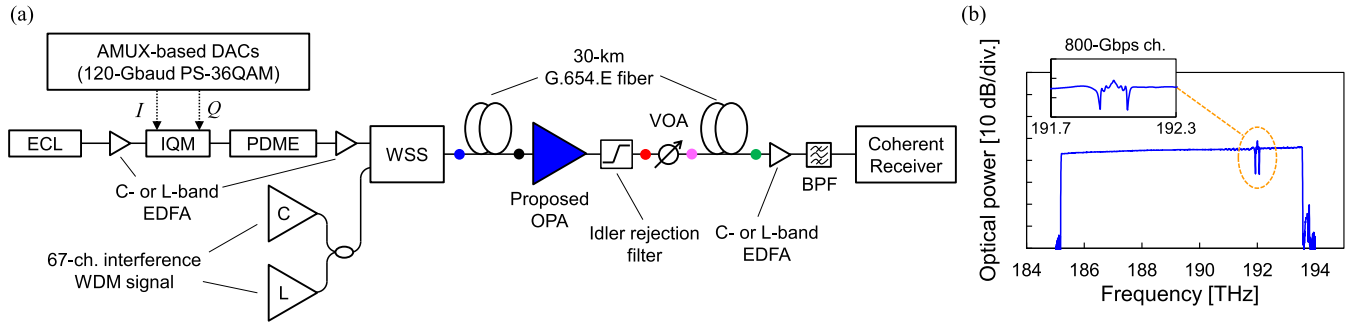

Fig. 6. Experimental setup for 2×30-km 8.375-THz WDM transmission. (a) Link configuration. Color dots indicate points at which optical spectra shown in Fig. 7 were measured. (b) Spectrum of launched 8.375-THz WDM signal (0.1-nm resolution).

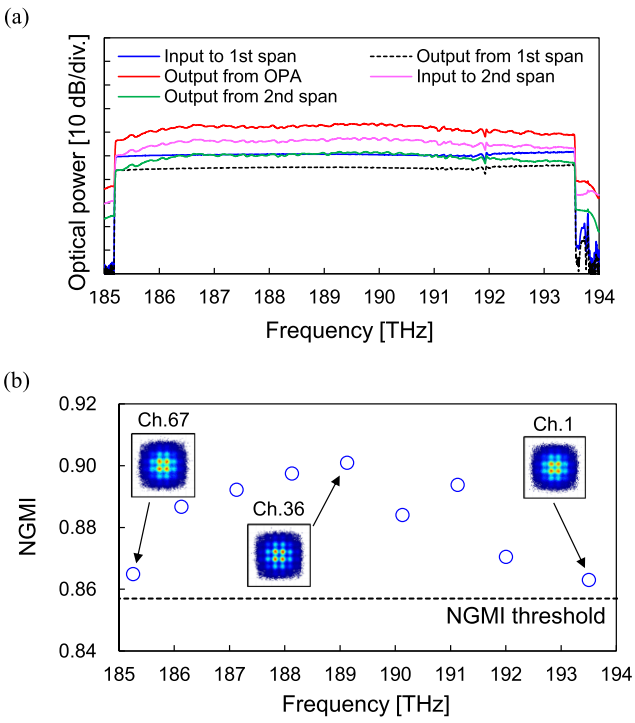

Fig. 7. Experimental results. (a) Spectra of WDM signal at each point (0.1-nm resolution). (b) NGMI characteristics of representative channels.

calculated from the demodulated signal. Assuming the concatenated coding of low-density parity-check code and BCH code with a code rate of 0.826 and a 1.64% pilot symbol inserted in the signal data, the net data rate per channel was 800 Gbps with a NGMI threshold of 0.857 [14].

B. Results

Fig. 7(a) shows the optical spectra at each point. The output spectra from the OPA indicated that the gain of the OPA was sufficient for compensating for the transmission loss of the 30-km fiber. The optical attenuation before the 2nd span was set so that the input power to each span at a frequency with the lowest gain was the same. Since we did not perform gain equalization, the WDM signal input to the 2nd span had a spectral gradient caused by the gain spectrum of the OPA. We tested only nine representative channels to verify the basic characteristics of the inline-amplified transmission with the proposed OPA. Fig. 7(b) shows the NGMI characteristics. All measured channels were better than the NGMI threshold. The frequency dependence of the NGMI corresponded to the gain spectrum of the OPA. This result is reasonable because the optical signal-to-noise ratio of each channel was different depending on the input power to the 2nd span. The NGMI characteristics and constellation were generally linear as expected, and no excess signal distortion due to cascading PPLNs and reusing the pump was observed in the gain-unsaturated region.

V. Conclusion

We proposed a configuration for optical parametric amplification using cascaded PPLN modules with reused pump light. The cascaded PPLNs have complementary gain profiles, and reusing the pump light makes extending the power-efficient gain bandwidth possible. We experimentally showed a 0.9-THz (8-nm) bandwidth extension without pump-power enhancement in comparison with a conventional PPLN-based OPA. As a result, an 8.7-THz-gain bandwidth was achieved from the degenerate frequency with a >15-dB gain. In addition, numerical analysis based on the CWE showed that the temperature detuning of the 2nd PPLNs can suppress unwanted excessive gain and improve the flatness of the gain spectrum. We also demonstrated 8.375-THz optical inline amplification of a WDM signal using the proposed OPA under a 2 × 30-km transmission condition.

This work utilized only the lower frequency band of the OPA from the degenerate frequency. The experimental results showed that the PPLN-based OPA has a potential >17-THz amplification bandwidth including a guard band around the degenerate frequency by using both the upper and lower bands with a full-band configuration [16]. It is also possible to use it as an ultra-wideband wavelength converter of >8-THz bandwidth using idler light. In this work, the proposed OPA was configured by connecting 4-port PPLN modules with fiber pigtails and connectors as a proof-of-concept. To achieve higher efficiency, the optical loss of the signal and pump lights between two PPLN waveguides should be reduced. For example, it is effective to integrate two waveguides into a single module. A wider

extension could be achieved by reducing the excessive optical loss in the proposed configuration, especially that of the pump line that effects the efficiency of reusing the pump.

REFERENCES

[1] F. Hamaoka, M. Nakamura, M. Takahashi, T. Kobayashi, Y. Miyamoto, and Y. Kisaka, "173.7-Tb/s triple-band WDM transmission using 124-channel 144-gbaud signals with SE of 9.33 b/s/Hz," in *Proc. Opt. Fiber Commun. Conf.*, 2023, Paper Th3F.2.

[2] B. J. Puttnam, R. S. Luís, G. Rademacher, M. Mendez-Astudillio, Y. Awaji, and H. Furukawa, "S-, C- and L-band transmission over a 157 nm bandwidth using doped fiber and distributed Raman amplification," *Opt. Exp.*, vol. 30, no. 6, pp. 10011–10018, Mar. 2022.

[3] X. Zhao et al., "200.5 Tb/s transmission with S+C+L amplification covering 150 nm bandwidth over 2×100 km PSCF Spans," in *Proc. Eur. Conf. Opt. Commun.*, 2022, Paper Th3C.4.

[4] F. Pittalà et al., "72.64 Tb/s DWDM transmission over 100 km G.654D fiber using super C-band erbium-doped fiber amplification," in *Proc. Opt. Fiber Commun. Conf.*, 2022, Paper W3C.4.

[5] J. Renaudier et al., "First 100-nm continuous-band WDM transmission system with 115Tb/s transport over 100km using novel ultra-wideband semiconductor optical amplifiers," in *Proc. Eur. Conf. Opt. Commun.*, 2017, Paper Th.PDP.A.2.

[6] H. Masuda et al., "20.4-Tb/s (204 × 111 Gb/s) transmission over 240 km using bandwidth-maximized hybrid Raman/EDFAs," in *Proc. Opt. Fiber Commun. Conf.*, 2007, Paper PDP20.

[7] M. Ionescu et al., "74.38 Tb/s transmission over 6300 km single mode fiber with hybrid EDFA/Raman amplifiers," in *Proc. Opt. Fiber Commun. Conf.*, 2019, Paper Tu3F.3.

[8] F. Hamaoka et al., "Ultra-wideband WDM transmission in S-, C-, and L-bands using signal power optimization scheme," *J. Lightw. Technol.*, vol. 37, no. 8, pp. 1764–1771, Apr. 2019.

[9] R. Malik, A. Kumpera, M. Karlsson, and P. A. Andrekson, "Demonstration of ultra wideband phase-sensitive fiber optical parametric amplifier," *Photon. Technol. Lett.*, vol. 28, no. 2, pp. 175–177, Jan. 2015.

[10] C. B. Gaur, V. Gordienko, P. Hazarika, and N. J. Doran, "Polarization Insensitive fiber optic parametric amplifier with a gain bandwidth of 22 nm in S-band," in *Proc. Opt. Fiber Commun. Conf.*, 2022, Paper W4J.1.

[11] T. Kato et al., "Real-time transmission of 240×200-Gb/s signal in S+C+L triple-band WDM without S- or L-band transceivers," in *Proc. Eur. Conf. Opt. Commun.*, 2019, Paper PD.1.7.

[12] T. Kato et al., "S+C+L-band WDM transmission using 400-Gb/s real-time transceivers extended by PPLN-based wavelength converter," in *Proc. Eur. Conf. Opt. Commun.*, 2022, Paper We4D.4.

[13] S. Shimizu et al., "PPLN-based optical parametric amplification for wideband WDM transmission," *J. Lightw. Technol.*, vol. 40, no. 11, pp. 3374–3384, Jun. 2022.

[14] T. Kobayashi et al., "Wide-band inline-amplified WDM transmission using PPLN-based optical parametric amplifier," *J. Lightw. Technol.*, vol. 39, no. 3, pp. 787–794, Feb. 2021.

[15] T. Kobayashi et al., "50-Tb/s (1 Tb/s × 50 ch) WDM transmission on two 6.25-THz bands using hybrid inline repeater of PPLN-based OPAs and incoherent-forward-pumped DRA," in *Proc. Opt. Fiber Commun. Conf.*, 2022, Paper Th4A.8.

[16] T. Kobayashi et al., "103-ch. 132-Gbaud PS-QAM signal inline-amplified transmission with 14.1-THz bandwidth lumped PPLN-based OPAs Over 400-km G.652.D SMF," in *Proc. Opt. Fiber Commun. Conf.*, 2023, Paper Th4B.6.

[17] S. Shimizu et al., "8.375-THz optical amplification for wideband WDM transmission by optical parametric amplifier using cascaded PPLN modules with complementary gain profiles," in *Proc. Eur. Conf. Opt. Commun.*, 2022, Paper We4D.1.

[18] T. Kazama et al., "Over-30-dB gain and 1-dB noise figure phase-sensitive amplification using pump-combiner-integrated fiber I/O PPLN module," *Opt. Exp.*, vol. 29, no. 18, pp. 28824–28834, Aug. 2021.

[19] T. Kashiwazaki, T. Yamashima, N. Takanashi, A. Inoue, T. Umeki, and A. Furusawa, "Fabrication of low-loss quasi-single-mode PPLN waveguide and its application to a modularized broadband high-level squeezer," *Appl. Phys. Lett.*, vol. 119, Dec. 2021, Art. no. 251104.

[20] T. Kazama, T. Umeki, M. Abe, K. Enbutsu, Y. Miyamoto, and H. Takenouchi, "Low-parametric-crosstalk phase-sensitive amplifier for guard-band-less DWDM signal using PPLN waveguides," *J. Lightw. Technol.*, vol. 35, no. 4, pp. 755–761, Feb. 2017.

[21] R. W. Boyd, *Nonlinear Optics*, 4th ed. Amsterdam, The Netherlands: Elsevier, 2020.

[22] T. Yanagawa et al., "Simultaneous observation of CO isotopomer absorption by broadband difference-frequency generation using a direct-bonded quasi-phase-matched $LiNbO_3$ waveguide," *Opt. Lett.*, vol. 31, no. 7, pp. 960–962, Apr. 2006.

[23] D. H. Jundt, "Temperature-dependent Sellmeier equation for the index of refraction, n_e, in congruent lithium niobate," *Opt. Lett.*, vol. 22, no. 20, pp. 1553–1555, Oct. 1997.

[24] K. Inoue and T. Mukai, "Signal wavelength dependence of gain saturation in a fiber optical parametric amplifier," *Opt. Lett.*, vol. 26, no. 1, pp. 10–12, Jan. 2001.

[25] K. Inoue, "Analysis of quantum noise of a gain-saturated fiber-based optical parametric amplifier based on an equivalent input noise model," *J. Opt. Soc. Amer. B*, vol. 37, no. 11, pp. 3251–3260, Nov. 2020.

[26] M. Asobe, T. Umeki, and O. Tadanaga, "Phase sensitive amplification with noise figure below the 3 dB quantum limit using CW pumped PPLN waveguide," *Opt. Exp.*, vol. 20, no. 12, pp. 13164–13172, May 2012.

[27] F. Hamaoka et al., "120-GBaud 32QAM signal generation using ultra-broadband electrical bandwidth doubler," in *Proc. Opt. Fiber Commun. Conf.*, 2019, Paper M2H.6.

[28] D. J. Elson et al., "Investigation of bandwidth loading in optical fibre transmission using amplified spontaneous emission noise," *Opt. Exp.*, vol. 25, no. 16, pp. 19529–19537, Aug. 2017.

[29] F. Bessin, V. Gordienko, F. M. Ferreira, and N. Doran, "First experimental Mach-Zehnder FOPA for polarization- and wavelength-division-multiplexed signals," in *Proc. Eur. Conf. Opt. Commun.*, 2021, pp. 1–3.

[30] T. Kobayashi et al., "35-Tb/s C-band transmission over 800 km employing 1-Tb/s PS-64QAM signals enhanced by complex 8×2 MIMO equalizer," in *Proc. Opt. Fiber Commun. Conf.*, 2019, Paper Th4B.2.

Shimpei Shimizu (Member, IEEE) received the B.E. degree in engineering and the M.E. degree in information science and technology in the field of electronics for informatics from Hokkaido University, Sapporo, Japan, in 2016 and 2018, respectively. In 2018, he joined the NTT Network Innovation Laboratories, Yokosuka, Japan. His research focuses on high-capacity optical transmission systems. He is currently the Member of the Institute of Electronics, Information and Communication Engineers (IEICE) of Japan and IEEE Photonics Society.

Takayuki Kobayashi (Member, IEEE) received the B.E., M.E., and Dr. Eng. degrees from Waseda University, Tokyo, Japan, in 2004, 2006, and 2019, respectively. In 2006, he joined the NTT Network Innovation Laboratories, Yokosuka, Japan, where he researched on high-speed and high-capacity digital coherent transmission systems. In 2014, he moved to the NTT Access Network Service Systems Laboratories, Yokosuka, and was with 5G Mobile Optical Network Systems. Since 2016, he has been with NTT Network Innovation Laboratories, working on high-capacity optical transmission systems. His research interests include long-haul optical transmission systems employing spectrally efficient modulation formats enhanced by digital and optical signal processing. He is currently the Member of the Institute of Electronics, Information and Communication Engineers (IEICE) of Japan. From 2016 to 2018, he was a Technical Program Committee (TPC) Member of the Electrical Subsystems' Category for the Optical Fiber Communication Conference (OFC). Since 2018, he has been the TPC Member of the "Point-to-Point Optical Transmission" Category for the European Conference on Optical Communication (ECOC).

Takushi Kazama received the B.S. and M.S. degrees in electrical engineering from The University of Tokyo, Tokyo, Japan, in 2009 and 2011, respectively. In 2011, he joined the NTT Device Technology Laboratories, Japan, where he researched on nonlinear optical devices based on periodically poled $LiNbO_3$ waveguides. He is the Member of the Institute of Electronics, Information, and Communication Engineers of Japan (IEICE) and the Japan Society of Applied Physics (JSAP).

Takeshi Umeki (Member, IEEE) received the B.S. degree in physics from Gakushuin University, Tokyo, Japan, in 2002, the M.S. degree in physics and the Ph.D. degree in nonlinear optics from The University of Tokyo, Tokyo, in 2004 and 2014, respectively. In 2004, he joined the NTT Photonics Laboratories, Atsugi, Japan, where he researched on nonlinear optical devices based on periodically poled $LiNbO_3$ waveguides. He is the Member of the Japan Society of Applied Physics (JSAP), Institute of Electronics, Information, and Communication Engineers (IEICE), and the IEEE/Photonics Society.

Masanori Nakamura (Member, IEEE) received the B.S. and M.S. degrees in applied physics from Waseda University, Tokyo, Japan, in 2011 and 2013, respectively, and the Ph.D. degrees in electrical, electronic, and infocommunications engineering from Osaka University, Osaka, Japan, in 2021. In 2013, he joined NTT Network Innovation Laboratories, Yokosuka, Japan, where he researched on high-capacity optical transport networks. He was the recipient of the 2016 IEICE Communications Society Optical Communication Systems Young Researchers Award. He is the Member of the Institute of Electronics, Information and Communication Engineers, Tokyo, Japan.

Koji Enbutsu received the B.E. and M.E. degrees in electronics engineering from Hokkaido University, Sapporo, Japan, in 1994 and 1996, respectively. In 1996, he joined the NTT Opto-Electronics Laboratories, Japan, where he researched on organic optical waveguides for optical communications and electro-optic crystals and their devices. In 2007, he moved to the NTT Access Services Network System Laboratories, where he researched on optical fiber testing and monitoring. He is the Member of the Institute of Electronics, Information, and Communication Engineers (IEICE) and the Japan Society of Applied Physics (JSAP).

Takahiro Kashiwazaki received the B.E. and M.E. degrees in materials science from Keio University, Japan, in 2013 and 2015, respectively. In 2015, he joined the NTT Device Technology Laboratories, Atsugi, Japan. He is currently researching on periodically poled lithium niobate waveguide devices. He is also the Member of the Institute of Electronics, Information, and Communication Engineers of Japan (IEICE) and the Japan Society of Applied Physics (JSAP).

Fukutaro Hamaoka (Member, IEEE) received the B.E., M.E., and Ph.D. degrees in electrical engineering from Keio University, Yokohama, Japan, in 2005, 2006, and 2009, respectively. From 2009 to 2014, he was with NTT Network Service Systems Laboratories, Musashino, Japan, where he was with the Research and Development of high-speed optical communication systems, including digital coherent optical transmission system. He is currently with NTT Network Innovation Laboratories, Yokosuka, Japan. His research interests include high-capacity optical transport systems with ultra-wideband wavelength division multiplexing and high symbol rate techniques. Dr. Hamaoka is the Member of the Institute of Electronics, Information, and Communication Engineers (IEICE) of Japan. He was the recipient of the 2007 The Japan Society of Applied Physics Young Scientist Presentation Award.

Munehiko Nagatani (Member, IEEE) received the M.S. and Ph.D. degrees in electrical and electronics engineering from Sophia University, Tokyo, Japan, in 2007 and 2021, respectively. In 2007, he joined NTT Photonics Laboratories, NTT Corporation, where he was with the R&D of ultrahigh-speed mixed signal ICs for optical communications systems. He is currently with NTT Network Innovation Laboratories and NTT Device Technology Laboratories, where he was with the R&D of extreme-broadband analog ICs for communications and emerging applications. He is also the Member of the Institute of Electronics, Information and Communication Engineers (IEICE) of Japan.

Hiroshi Yamazaki (Member, IEEE) received the B.S. degree in integrated human studies and the M.S. degree in human and environmental studies from Kyoto University, Kyoto, Japan, in 2003 and 2005, respectively, and the Dr. Eng. degree in electronics and applied physics from the Tokyo Institute of Technology, Tokyo, Japan, in 2015. In 2005, he joined NTT Photonics Laboratories, Kanagawa, Japan, where he researched on optical waveguide devices for communications systems. He is concurrently with NTT Network Innovation Laboratories and NTT Device Technology Laboratories, Kanagawa, Japan, where he researched on devices and systems for optical transmission using advanced multilevel modulation formats. He is also the Member of the Institute of Electronics, Information and Communication Engineers of Japan.

Kei Watanabe received the B.E., M.E., and Dr. Eng. degrees in physical electronics from Kobe University, Kobe, Japan, in 1998, 2000, and 2003, respectively. In 2004, he joined NTT Laboratories, Kanagawa, Japan, where he researched on silica-based optical waveguides. From 2008 to 2009, he was with Photonic Research Group, Ghent University, Ghent, Belgium, as a Visiting Researcher, where he focused on uniting silicon photonics and silica-based optical waveguides. Since 2009, he has been with the Development of InP-based high-speed Mach–Zehnder modulators. He is the Member of the Japan Society of Applied Physics, the Institute of Electronics, Information, and Communication Engineers of Japan, and the IEEE Photonics Society.

Yutaka Miyamoto (Member, IEEE) received the B.E. and M.E. degrees in electrical engineering from Waseda University, Tokyo, Japan, in 1986 and 1988, respectively, and the Dr. Eng. degree in electrical engineering from Tokyo University, Tokyo, in 2016. In 1988, he joined the NTT Transmission Systems Laboratories, Yokosuka, Japan, where he was with the Research and Development of highspeed optical communications systems including the 10-Gbit/s first terrestrial optical transmission system (FA-10G) using erbium-doped fiber amplifiers (EDFA) inline repeaters. From 1995 to 1997, he was with the NTT Electronics Technology Corporation, Yokohama, Japan, where he was with the Planning and Product Development of high-speed optical module at the data rate of 10 Gb/s and beyond. Since 1997, he has been with the NTT Network Innovation Laboratories, Yokosuka, Japan, where he with the Research and Development of optical transport technologies based on 40/100/400-Gbit/s channel and beyond. He is currently an NTT Fellow and the Director of the Innovative Photonic Network Research Center, NTT Network Innovation Laboratories, where he is investigating and promoting the future scalable optical transport network with the Pbit/s-class capacity based on innovative transport technologies such as digital signal processing, space division multiplexing, and cutting-edge integrated devices for photonic preprocessing. He is also the Fellow of the Institute of Electronics, Information and Communication Engineers (IEICE).